Macromolecules

Article

pubs.acs.org/Macromolecules

Photovoltaic Performance of Block Copolymer Devices Is Independent of the Crystalline Texture in the Active Layer

Changhe Guo,[†] Youngmin Lee,[†] Yen-Hao Lin,[∥] Joseph Strzalka,[⊥] Cheng Wang,[#] Alexander Hexemer,[#] Cherno Jaye,[%] Daniel A. Fischer,[%] Rafael Verduzco,[∥] Qing Wang,[§] and Enrique D. Gomez*[,†,‡]

[†]Department of Chemical Engineering, [‡]Materials Research Institute, and [§]Department of Materials Science and Engineering, The Pennsylvania State University, University Park, Pennsylvania 16802, United States

[∥]Department of Chemical and Biomolecular Engineering, Rice University, Houston, Texas 77005, United States

[⊥]X-ray Science Division, Argonne National Laboratory, Argonne, Illinois 60439, United States

[#]Advanced Light Source, Lawrence Berkeley National Laboratory, Berkeley, California 94720, United States

[%]Materials Science and Engineering Laboratory, National Institute of Standards and Technology, Gaithersburg, Maryland 20899, United States

Supporting Information

ABSTRACT: The electronic properties of organic semiconductors are strongly influenced by intermolecular packing. When cast as thin films, crystalline π-conjugated molecules are strongly textured, potentially leading to anisotropic charge transport. Consequently, it is hypothesized that the orientation of crystallites in the active layer plays an important role in charge extraction and organic photovoltaic device performance. Here we demonstrate orientation control of molecular packing from mostly face-on to edge-on configurations in the active layer of P3HT-*b*-PFTBT block copolymer photovoltaics using 1-chloronaphthalene as a solvent additive. The effect of molecular orientations in P3HT crystals on charge transport and solar cell performance is examined. We find that optimized photovoltaic device performance is independent of the crystalline texture of P3HT. Our observations provide further insights into the molecular organization required for efficient charge transport and overall device efficiencies. The dominant crystal orientation, whether face-on or edge-on, is not critical to block copolymer solar cells. Instead, a broad distribution of crystallite orientations ensures pathways for charge transport in any direction and enables efficient charge extraction in photovoltaic devices.

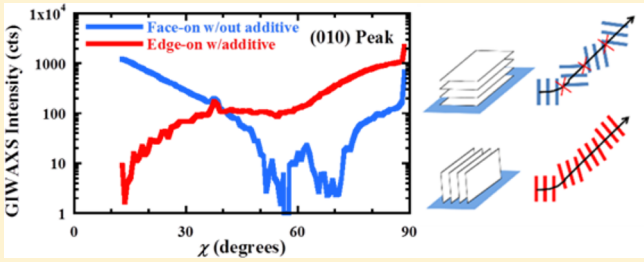

INTRODUCTION

Conjugated polymers have emerged as promising functional materials for solution-processable organic photovoltaics, with great potential to produce large-scale and renewable power in the form of flexible electronic devices.[1−3] Efficient power conversion in organic photovoltaics requires optimization of a series of processes related to light absorption, exciton diffusion, charge separation, and charge transport; the latter three are strongly dependent on the microstructure within the active layer. A common approach is to utilize a bulk heterojunction architecture, where electron donor and acceptor materials form an interpenetrating network of nanoscale domains, to create interconnected pathways for charge transport and large interfacial area for exciton dissociation into charge-separated states.[4−12] Extensive efforts have been devoted to tuning the microstructure in commonly utilized polymer/fullerene mixtures, leading to great progress in organic photovoltaic device performance.[13−22]

In addition to control over the mesoscale morphology, molecular order within nanoscale domains could significantly impact organic photovoltaic device performance as well. It is hypothesized that the molecular orientation of π-conjugated molecules can greatly influence optoelectronic properties. For example, differences by orders of magnitude in charge mobilities of poly(3-hexylthiophene-2,5-diyl) (P3HT), a commonly used donor polymer in solar cells, have been attributed to differences in molecular order in the active layer.[23,24] Regioregular P3HT self-organizes into a crystalline structure through $\pi-\pi$ interchain stacking of conjugated thiophene rings and segregation of alkyl side chains to spaces in between the polymer backbones.[25] In studies of P3HT field-effect transistors (FETs),[23] in-plane hole mobilities near 0.1 $cm^2\ V^{-1}\ s^{-1}$ from devices are correlated to $\pi-\pi$ stacking parallel to the substrate ("edge-on" orientation) in the active layer. If the dominant orientation is "face-on" in the active layer, where the overlap of π-orbitals is perpendicular and stacking of polymer side chains are aligned with the substrate, the in-plane mobility of devices decreases by several orders of magnitude.

Received: February 20, 2016
Revised: May 13, 2016
Published: June 15, 2016

DOI: 10.1021/acs.macromol.6b00370
Macromolecules 2016, 49, 4599−4608

Because charge transport is fast along the $\pi-\pi$ stacking direction, it is generally surmised in solar cell architectures that face-on orientations in the active layer are favorable for out-of-plane charge transport to the corresponding electrodes and overall device performance.[26−29]

Many reports have explored control of molecular packing toward face-on orientations through an optimization of processing conditions including choice of solvents,[25] the application of solvent additives,[17] thermal treatment,[30] and surface modification,[31,32] or through chemical strategies such as tuning polymer regioregularity[23] and side chain engineering.[33] Recently, such face-on orientations have been induced in polymer/fullerene mixtures and are perceived as contributing to enhanced charge transport and resulting high performance of polymer solar cells.[31,33] In most cases, however, the alignment of crystal orientation is inevitably associated with changes of the polymer/fullerene blend structures such as the degree of phase separation and domain connectivity. The inability to decouple these mesoscale morphological factors gives rise to a challenge in directly correlating molecular organization with device performance. In addition, recent work suggests that the orientation between donor and acceptor materials can also tune the electronic coupling across the interface and thus affect charge generation.[26,34−36] This further complicates efforts to elucidate the role of molecular orientation, or the texturing of crystallites, in the active layer of organic photovoltaics.

Here we examine the effect of crystalline texture on the photovoltaic performance of conjugated donor−acceptor block copolymer solar cells composed of poly(3-hexylthiophene-2,5-diyl)-*block*-poly((9,9-bis(2-octyl)fluorene-2,7-diyl)-*alt*-(4,7-di-(thiophene-2-yl)-2,1,3-benzothiadiazole-5′,5″-diyl)) (P3HT-*b*-PFTBT) as the active layer. Previously, we have demonstrated that the self-assembly of P3HT-*b*-PFTBT block copolymers into nanoscale lamellar morphologies leads to power conversion efficiencies of 2.7%.[37] The well-defined microstructure and covalently linked donor−acceptor heterojunctions allow us to focus on the influence of molecular packing, particularly in crystalline P3HT, on photoconversion efficiencies (PCEs) of block copolymer solar cells. We employ solution processing with a solvent additive 1-chloronaphthalene to induce a texture change from mostly face-on to edge-on orientations in the crystalline P3HT block, while the PFTBT block remains amorphous. No distinct differences in the self-assembled structures are observed after the application of solvent additives as characterized by resonant soft X-ray scattering (RSOXS). Surprisingly, we find that the dramatic change in crystalline orientations results in very similar device performance of optimized block copolymer solar cells, implying that block copolymer photovoltaic performance is independent of the crystalline texture in the active layer. We hypothesize that the ubiquitous broad distribution of crystallite orientations present in polymeric semiconductors creates percolating pathways for charge transport through tie chains, even when the average orientation is not favorable for charge transport in the desired direction.

■ MATERIALS AND METHODS

P3HT-*b*-PFTBT block copolymers were synthesized using a similar procedure as described in ref 37.

Photovoltaic devices were prepared with the conventional architecture of ITO/PEDOT:PSS (70 nm)/active layer (65−85 nm)/Al (75 nm). ITO-coated glass substrates (20 ohm/sq, Xin Yan Technology, Hong Kong) were cleaned by soap, followed by 20 min of sonication in acetone, then isopropanol, and finally 15 min of ultraviolet light ozonation. Poly(3,4-ethylenedioxythiophene):poly-(styrenesulfonate), PEDOT:PSS (Clevios P, Heraeus), was spin-coated on top of ITO at 4000 rpm for 2 min yielding a thickness of about 70 nm. The PEDOT:PSS/ITO substrates were dried for 10 min at 165 °C in air and then transferred to a nitrogen-filled glovebox. Solutions of P3HT-*b*-PFTBT (5 mg/mL) were made with anhydrous chloroform (≥99%, amylenes as stabilizer, Sigma-Aldrich) and stirred at 95 °C for about 20 h in a tightly sealed container in the N_2 glovebox. Solutions were filtrated with a 0.2 μm filter and stirred for another 2 h at 95 °C prior to casting. The active layers of P3HT-*b*-PFTBT devices were spin-cast onto PEDOT:PSS layers from prepared hot solutions (95 °C) at various spin speeds for 1 min to yield thicknesses around 65−85 nm. The film thicknesses were determined on a TENCOR P-10 surface profiler. Samples were then transferred immediately onto a calibrated digital hot plate at 165 °C and dried for 5 min. The devices were completed by vacuum thermal evaporation of 75 nm aluminum at 10^{-6} Torr on top of the active layer through a shadow mask. The device area is 16.2 mm^2. Integrated solar cells were further annealed at 165 °C for various annealing times until the maximum device performance was recorded. Optimum device performance was found after annealing for 10 min.

Photovoltaic measurements were performed in a N_2-filled atmosphere under simulated AM 1.5G illumination (95 mW/cm^2) from a xenon lamp solar simulator (Newport Model SP92250A-1000). The illumination intensity was calibrated using an optical power meter and NREL certified Si reference photocell (Newport). A Keithley 2636A SourceMeter was used to measure the current−voltage characteristics of solar cells. The absorption spectra of films were measured using an ultraviolet/visible/near-infrared spectrophotometer (Beckman DU Series 500).

Samples for RSOXS and GIWAXS measurements were prepared on PEDOT:PSS/Si substrates in the same manner as for device fabrication. For RSOXS experiments, as-cast films were floated-off in deionized water and picked up with 5 mm × 5 mm silicon frames supporting a 1 mm × 1 mm, 100 nm thick Si_3N_4 window. Samples were then dried for 24 h at room temperature under vacuum and subsequently annealed on a hot plate in the N_2 glovebox.

RSOXS measurements were carried out at beamline 11.0.1.2 at the Advanced Light Source, Lawrence Berkeley National Laboratory. Scattering was performed in the transmission geometry in vacuum at X-ray energies at the carbon absorption edge (285.4 eV) with linearly polarized X-rays. Data were corrected for dark currents and azimuthally integrated.

GIWAXS measurements were carried out at Beamline 8-ID-E of the Advanced Photon Source, Argonne National Laboratory (λ = 1.6868 Å).[38] Scattering data were acquired at an incident angle of 0.2°. Data are corrected for X-ray polarization, detector sensitivity, and geometrical solid-angle.[39] GIWAXS intensities are integrated over a q window of ±0.06 $Å^{-1}$ around the (100) peak at 0.36 $Å^{-1}$ and ±0.10 $Å^{-1}$ range around the (010) reflection at 1.65 $Å^{-1}$. A linear background was subtracted from the integrated data using intensities away from the Bragg peak of interest.

NEXAFS measurements were carried out at the NIST/Dow soft X-ray materials characterization beamline U7A of the National Synchrotron Light Source at Brookhaven National Laboratories. Partial electron yield (PEY) NEXAFS spectra were acquired at the carbon K-edge at different incident angles. Data are normalized by the corresponding incident beam intensity and postedge values (320 eV) of the spectra.

■ RESULTS AND DISCUSSION

Previous X-ray diffraction studies have shown that P3HT-*b*-PFTBT (Figure 1a) is a crystalline−amorphous conjugated block copolymer where the PFTBT block is amorphous or weakly crystalline, while the P3HT block crystallizes with the same characteristic diffraction peaks (h00) as that in neat P3HT films.[37,40] No measurable changes in the lattice spacing are observed, suggesting that cocrystallization of P3HT with

DOI: 10.1021/acs.macromol.6b00370
Macromolecules 2016, 49, 4599−4608

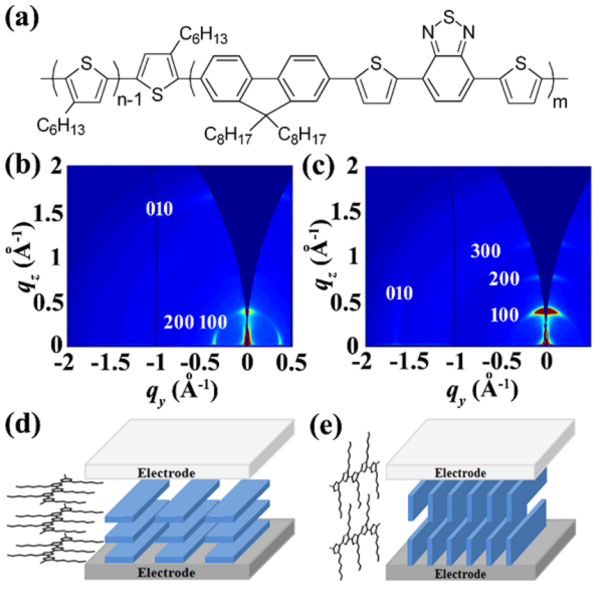

Figure 1. (a) Chemical structure of P3HT-*b*-PFTBT. (b, c) Two-dimensional grazing-incidence wide-angle X-ray scattering (GIWAXS) data of P3HT-*b*-PFTBT films cast from solutions without 1-chloronaphthalene (b) and with 5% 1-chloronaphthalene as a solvent additive (c). All samples were annealed at 165 °C for 10 min. (d, e) Schematic illustrations for π-stacking within P3HT domains denoting the molecular orientation for P3HT-*b*-PFTBT films cast from solutions without a solvent additive (d) and cast from 5% 1-chloronaphthalene solutions (e). Block copolymer films cast without solvent additive adopt predominant face-on orientations with out-of-plane π-stacking in P3HT domains. When the solvent additive is used, P3HT crystals demonstrate a dramatic change in molecular packing from face-on to edge-on orientations.

PFTBT does not exist to any measurable degree. Details of the crystallographic texture in the P3HT block were examined using grazing-incidence wide-angle X-ray scattering (GIWAXS). Experiments were performed on block copolymer thin films deposited on PEDOT:PSS-coated Si substrates to simulate identical surface conditions as in the solar cell architecture and annealed in an analogous manner (165 °C) to optimized devices; annealing at 165 °C for 10 min maximizes crystallinity of the P3HT block. Two-dimensional GIWAXS measurements probe the preferred crystal orientations through analysis of the scattering patterns in both in-plane (q_y) and out-of-plane (q_z) directions.

Figures 1b and 1c compare the GIWAXS data of P3HT-*b*-PFTBT thin films spun-cast from chloroform solutions with 0 and 5 vol % of 1-chloronaphthalene additives. For the block copolymer films with no additives (Figure 1b), the (010) diffraction peak of P3HT ($q \sim 1.65$ Å^{-1}) associated with the $\pi-\pi$ stacking reflection is only evident in the out-of-plane (along q_z) direction. Meanwhile, three orders of (h00) reflections ($q \sim 0.36$, 0.72, and 1.08 Å^{-1}), which correspond to the distance between P3HT backbones separated by the alkyl side chains, are apparent in-plane (along q_y) with the substrate. We note that the (100) peak is also visible in the surface normal direction, but with a minor population as discussed below in the orientation distribution of the (100) reflection (Figure 2a). This indicates that P3HT crystals in block copolymer films are mostly aligned face-on with $\pi-\pi$ stacking primarily normal to the substrate (or electrodes in devices) as illustrated in Figure 1d. This strong face-on packing differs from previously reported studies of P3HT crystallization in neat films or polymer mixtures where strong edge-on orientations are observed.[41−43]

After processing with 5% 1-chloronaphthalene additives, the crystalline texture is drastically different (Figure 1c). The (100), (200), and (300) peaks are highly oriented out-of-plane (along q_z), while the π-stacking peak (010) appears exclusively parallel to the substrate (along q_y), suggesting a predominant edge-on orientation (Figure 1e). The dominance of the edge-on orientation is apparent in the orientation distribution of the (010) reflection as shown in Figure 2b. Intensities were integrated over a q window of ±0.06 Å^{-1} for the (100) peak and ±0.10 Å^{-1} range for the (010) reflection. A linear background was subtracted from the integrated data using intensities away from the (100) peak. With the addition of 1-chloronaphthalene to the casting solution, P3HT-*b*-PFTBT films exhibit a significant increase of edge-on crystallites and a drastic drop in face-on population. Integrating the (100) intensities over all polar angles χ[44,45] suggests that the P3HT crystallinity increases by a factor of 2 when casting from 5% 1-chloronaphthalene solutions. Analysis of the peak widths reveals that the crystallite size along the (100) direction grows by a factor of 2 with the addition of 1-chloronaphthalene, although crystals do not grow along the (010) direction (see Table S1 of the Supporting Information). Nevertheless, Figure 2b shows that the (010) intensities, and therefore population of face-on crystallites, is more than 2 orders of magnitude lower in films cast from 5% 1-chloronaphthalene solutions.

Although we find no evidence of PFTBT crystallization in Figure 1, it is possible that a preferred PFTBT chain orientation exists near the substrate. A preferential orientation of the PFTBT block could affect the orientation of P3HT chains in

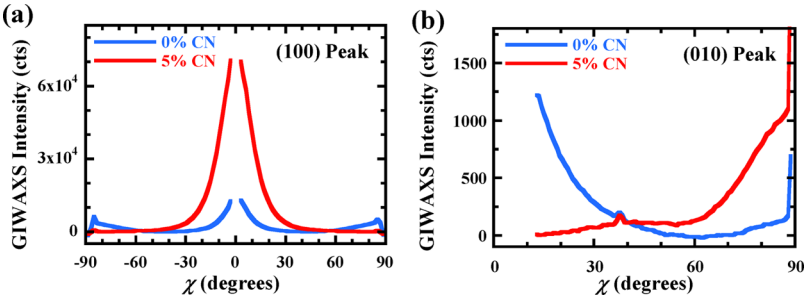

Figure 2. GIWAXS intensities as a function of χ, the polar angle in the plane of the 2D data, at P3HT (a) (100) and (b) (010) peaks for P3HT-*b*-PFTBT block copolymer thin films processed with 0% and 5% chloronaphthalene (CN) additives. $\chi = 0$ corresponds to the out-of-plane direction. Data are missing near $\chi = 0$ due to the grazing-incidence scattering geometry.

DOI: 10.1021/acs.macromol.6b00370
Macromolecules 2016, 49, 4599−4608

P3HT-*b*-PFTBT, thereby modulating the crystal orientation distribution. To examine the orientation of PFTBT chains, we used near-edge X-ray absorption fine structure (NEXAFS) spectroscopy on thin films (ca. 10 nm) of PFTBT homopolymers cast from solvents with and without 1-chloronaphthalene as a solvent additive. The films are thin to provide a measure of the molecular orientation near the substrate, given the 3−5 nm penetration depth of ∼280 eV X-rays.[46] Figures 3a and 3c show that the π^* peak at 285 eV

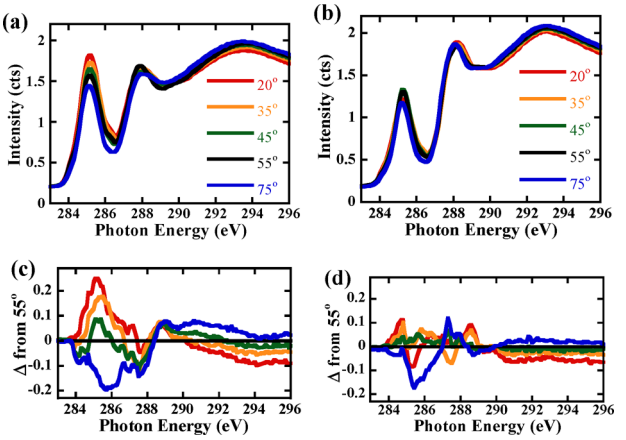

Figure 3. Angle-dependent postedge normalized NEXAFS spectra of PFTBT homopolymer cast from (a, c) chloroform or (b, d) 5 vol % 1-chloronaphthalene in chloroform. The difference spectra with 55° data as reference are plotted in (c) and (d). The films are very thin, ca. 10 nm, to examine chain orientations near the underlying substrate.

depends on the incident angle of the polarized X-rays, where the intensity decreases at higher angles. Thus, after casting from chloroform, π orbitals in PFTBT are preferentially aligned in the direction of the surface normal and chains are predominantly face-on.[47−49] Casting from the 1-chloronaphthalene/chloroform solution removes the dependence of the NEXAFS data on incident angle, suggesting that PFTBT is isotropic. Therefore, we speculate that 1-chloronaphthalene screens surface interactions between PFTBT and the substrate or promotes P3HT crystallization, allowing the P3HT block to form edge-on crystallites when casting the block copolymer.[31] Overall, adding a small amount of 1-chloronaphthalene into casting solutions leads to a dramatic change in the texture of P3HT crystals in P3HT-*b*-PFTBT block copolymer films, from a largely face-on packing without 1-chloronaphthalene to an edge-on orientation in crystalline P3HT domains when the additive is used.

Processing with solvent additives can not only tune the crystalline orientation but more often is applied to control mesoscale phase separation in polymer/fullerene mixtures.[17,18] Here we examine the effect of solvent additives on the self-assembled mesoscale structures in block copolymer thin films using resonant soft X-ray scattering (RSOXS). RSOXS is a powerful tool for structure characterization of polymer thin films with compositionally similar phases or in intricate multiphase systems.[50−52] Differences in the absorption in the soft X-ray range enable RSOXS to explore elemental and chemical contrast between different organic materials and provide greatly enhanced scattering intensities. The enhanced contrast in RSOXS over hard X-ray scattering techniques enables transmission geometries for scattering experiments of thin films, thereby allowing us to examine the in-plane morphology.

Figure 4 presents RSOXS scattering intensities as a function of in-plane scattering vector q ($q = 4\pi \sin(\theta/2)/\lambda$, λ is the X-ray

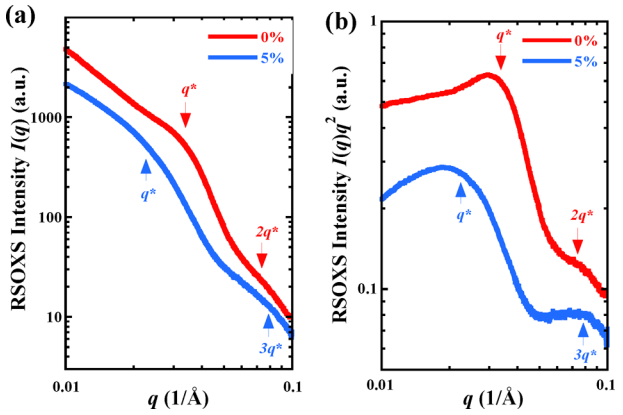

Figure 4. Comparison of the morphology in the active layers of P3HT-*b*-PFTBT photovoltaic devices processed with 0% and 5% solvent additive using RSOXS. RSOXS data were integrated over all polar angles and presented as (a) I vs q and (b) a Kratky plot of $I(q)q^2$ vs q, where $I(q)$ is the scattering intensity and q is the scattering vector. Scattering data were acquired at the carbon absorption edge of 285.4 eV. Scattering profiles are offset for comparisons. A primary scattering peak, q^*, and its higher-order reflections are identified for optimized P3HT-*b*-PFTBT samples with different concentrations of solvent additive.

wavelength and θ is the scattering angle) for thin films of P3HT-*b*-PFTBT block copolymers processed from chloroform or from 5% 1-chloronaphthalene in chloroform solutions. RSOXS experiments were performed at the carbon absorption edge of 285.4 eV, where significant absorption contrast exists between P3HT and PFTBT.[37] Films were annealed at the optimal conditions (165 °C for 10 min) for device performance. RSOXS data from P3HT-*b*-PFTBT thin films with and without 1-chloronaphthalene in the casting solvent show similar scattering patterns.

For block copolymer layers without the casting additive, a primary scattering peak at $q^* \approx 0.035$ Å^{-1} and a second-order reflection at $2q^*$ are evident. Higher order reflections are outside the q range for our experiments. Such scattering patterns in transmission experiments indicate an in-plane lamellar microstructure with an average domain spacing of approximately 18 nm. Each domain is approximately 9 nm in size, assuming a roughly symmetric composition of P3HT and PFTBT blocks. After the addition of 5% 1-chloronaphthalene to the casting solution, scattering data from the resulting films show a broad primary scattering feature at a slightly lower q (∼0.020 to 0.025 Å^{-1}), suggesting an increase in the structural periodicity with the domain size d of roughly 12−15 nm. The peak shift is clearly demonstrated in the Kratky plot (Iq^2 vs q) of RSOXS data as shown in Figure 4b. A third-order lamellar peak is now within the q range of our experiments and is visible at $3q^*$. The second-order reflection is not apparent and either may be enveloped into the broad initial peak or may be suppressed due to interference with the form factor for lamellae, as is common in block copolymers with symmetric compositions.[53,54] Nevertheless, peak intensities are roughly equivalent for both samples, such that the amount of lamellae perpendicular to the substrate remains the same for samples

DOI: 10.1021/acs.macromol.6b00370
Macromolecules 2016, 49, 4599−4608

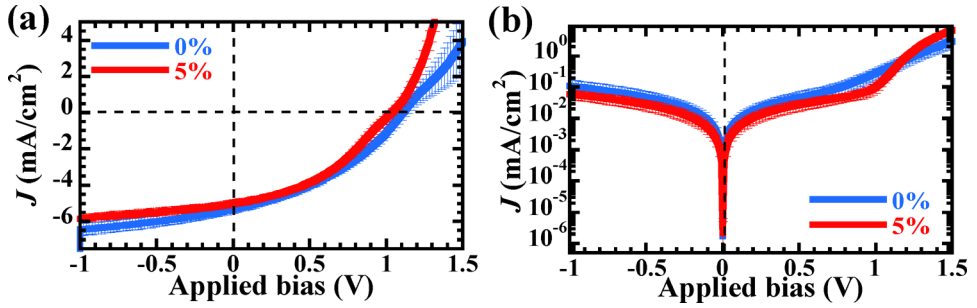

Figure 5. Average current−voltage characteristics of optimized P3HT-*b*-PFTBT photovoltaic devices processed with 0% and 5% solvent additive (a) under simulated 1 sun illumination and (b) in the dark. Data were averaged over six devices, and error bars denote the standard deviation. P3HT-*b*-PFTBT solar cells with different concentrations of solvent additives are both optimized at an annealing temperature of 165 °C.

cast from chloroform and from 5% 1-chloronaphthalene solutions.

The RSOXS data shown in Figure 4 suggest that P3HT-*b*-PFTBT with and without 1-chloronaphthalene in the casting solvent form in-plane lamellae with domain sizes of roughly 9−15 nm. We attribute the increase in the lamellar spacing after adding additives to the casting solution to swelling of domains by 1-chloronaphthalene during film deposition. Even if 1-chloronaphthalene leaves the film, it is not uncommon for block copolymers to be kinetically trapped at nonequilibrium domain sizes.[55−58] In most polymer semiconductors, excitons can only diffuse a short distance l_D (∼5−10 nm)[59] during their lifetime. Hence, the size of the domains should ideally be within the length scale of $2l_D$ (∼10−20 nm) in order to maximize the number of excitons that can reach the interface and undergo dissociation. Thus, the domain size (∼9 nm) is not limiting for exciton dissociation in block copolymer films cast without 1-chloronaphthalene, where donor/acceptor interfaces are always within the exciton diffusion length. When solvent additives are used, the slight increase in the lamellar domain size (∼12−15 nm) could prevent some excitons from reaching donor/acceptor interfaces. We estimate that at most 17−33% of excitons could be lost due to the larger than optimal domain sizes, assuming a short exciton diffusion length of 5 nm. In addition, we do not expect significant differences in the charge transfer process near the donor/acceptor junction when tuning the crystalline texture in the bulk domains. The relative orientation across donor and acceptor interfaces in conjugated P3HT-*b*-PFTBT block copolymers should be independent of the crystallite texture, as it is mainly governed by block copolymer self-assembly.[60] Therefore, the self-assembled microstructure of P3HT-*b*-PFTBT block copolymers provides an ideal model system to explicitly examine the impact of crystallite texturing on solar cell performance.

Average current−voltage (J−V) characteristics of P3HT-*b*-PFTBT block copolymer solar cells with distinct molecular orientations are compared in Figure 5, under 1 sun illumination (Figure 5a) as well as in the dark (Figure 5b). The block copolymer active layers were solution-processed without additive or with 5% 1-chloronaphthalene in the casting solvent in order to control the crystal texture of P3HT domains to either mostly face-on (0% 1-chloronaphthalene) or edge-on (5% 1-chloronaphthalene) orientations (Figure 1). All devices were fabricated in an ITO/PEDOT:PSS (70 nm)/P3HT-*b*-PFTBT (65−85 nm)/Al architecture and optimized at an annealing temperature of 165 °C. Regardless of whether 1-chloronaphthalene is used in the casting solution, optimized P3HT-*b*-PFTBT solar cells show similar photovoltaic responses under illumination (Figure 5a) and diode behaviors in the dark (Figure 5b). Some small differences are present at forward bias beyond V_{OC}. The device characteristics of optimal solar cell devices are summarized in Table 1.

Table 1. Device Characteristics[a] of Optimized P3HT-*b*-PFTBT Block Copolymer Solar Cells Processed with 0% and 5% Volume Fraction of 1-Chloronaphthalene

	efficiency (%)	short-circuit current (mA/cm²)	open-circuit voltage (V)	fill factor
0% additive	2.3 ± 0.2	5.3 ± 0.3	1.11 ± 0.03	0.38 ± 0.01
5% additive	2.2 ± 0.1	5.0 ± 0.2	1.04 ± 0.03	0.40 ± 0.01

[a]Under simulated AM 1.5G irradiation with intensity of 95 mW/cm².

In block copolymer devices with face-on P3HT crystals (0% 1-chloronaphthalene), an average power conversion efficiency (PCE) of 2.3 ± 0.2% with short-circuit currents (J_{SC}) of 5.3 ± 0.3 mA/cm², high open-circuit voltages (V_{OC}) of 1.11 ± 0.03, and fill factors of 0.38 ± 0.01 are obtained. Although the average device efficiency is slightly lower than the record of 2.7 ± 0.4% we previously reported for P3HT-*b*-PFTBT photovoltaics, the difference is not statistically significant.[37] Nevertheless, a lower performance could be due to variations in molecular weights and relative compositions of block copolymer materials synthesized from different batches. In this study, all solar cell devices were fabricated using materials from the same batch. Surprisingly, when the molecular packing in P3HT-*b*-PFTBT active layers changes from largely face-on (0% 1-chloronaphthalene) to edge-on (5% 1-chloronaphthalene) orientations, device characteristics (Table 1) including efficiency, J_{SC}, and fill factor are similar within statistical errors, although a slight drop in the average V_{OC} by about 70 mV (within 7%) in devices with edge-on P3HT crystals is observed. The origins for the differences in V_{OC} are currently unclear. Nevertheless, we conclude that the photovoltaic performance of P3HT-*b*-PFTBT block copolymer solar cells does not depend on the directions of the predominant crystal orientation in the active layer.

Although the difference in optimum performance is not statistically significant for devices made with and without 1-chloronaphthalene, the optimum active layer thicknesses to maximize P3HT-*b*-PFTBT photovoltaic device performance does differ. Block copolymer solar cells with face-on P3HT crystallites in the 65 nm thick active layer (0% 1-chloronaphthalene) exhibit an average PCE of 2.3 ± 0.2%, while a thicker active layer of 84 nm is needed to achieve similar

DOI: 10.1021/acs.macromol.6b00370
Macromolecules 2016, 49, 4599−4608

efficiencies of 2.2 ± 0.1% for P3HT-*b*-PFTBT devices composed of edge-on P3HT (5% 1-chloronaphthalene). The absorption spectra of different block copolymer films are compared in Figure S1 of the Supporting Information. For conjugated polymer films less than 100 nm, the absorption within devices is monotonic with film thickness.[61,62] Thus, optimal devices fabricated from solutions containing 5% 1-chloronaphthalene exhibit slightly higher absorptivity because the block copolymer film is thicker. Integrating the absorptivity results with an AM 1.5G solar spectrum predicts a small increase of approximately 9% in the number of absorbed photons. As a consequence, the similar short-circuit currents in optimized devices shown in Figure 5 suggests a slight drop in the internal quantum efficiency (IQE) for P3HT-*b*-PFTBT solar cells with primarily edge-on textures (5% 1-chloronaphthalene). This is consistent with excitonic losses due to the larger domain size (Figure 4) in block copolymer films after solvent additive treatment. One possibility is that more photons must be absorbed in the thicker active layer of additive-processed block copolymer solar cells in order to compensate for excitonic losses resulting from domain swelling with the solvent additive.

Moreover, P3HT-*b*-PFTBT solar cells with mostly edge-on P3HT crystals (5% 1-chloronaphthalene) in a thick active layer demonstrate a similar fill factor (Table 1) as that of devices with thinner active layers and mostly face-on P3HT textures (0% 1-chloronaphthalene). We further investigated the dependence of block copolymer photovoltaic performance on the thickness of the active layer.

As shown in Figure 6a, fill factors decrease with increasing film thicknesses in devices fabricated with and without 1-chloronaphthalene additives, suggesting that for thicker active layers performance is limited by charge extraction. More importantly, within the same thickness range, block copolymer solar cells show a near 30% increase in fill factors when the P3HT crystallite orientation is changing from mainly face-on (0% 1-chloronaphthalene) to edge-on (5% 1-chloronaphthalene). Also, the current at high forward bias is higher for devices composed of active layers with mostly edge-on P3HT (Figure 5). Given that PFTBT domains remain amorphous, the changes in fill factors and currents at high forward bias are most likely a result of the change in orientation of P3HT crystals. Therefore, our devices with mostly edge-on crystallite orientations demonstrate more efficient charge extraction than our solar cells with mainly face-on crystallites, even though we expect more efficient charge transport along the π-stacking direction.

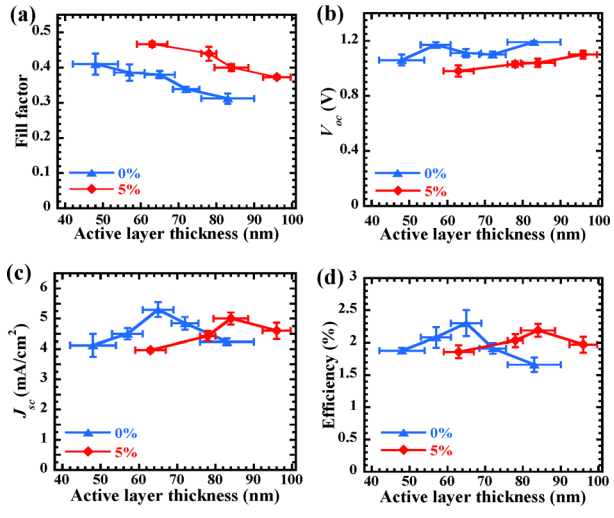

Figure 6. Photovoltaic performance for P3HT-*b*-PFTBT block copolymer solar cells processed with 0% and 5% solvent additives as a function of active layer thickness. (a) Fill factor, (b) open-circuit voltage, V_{OC}, (c) short-circuit current, J_{SC}, and (d) power conversion efficiency. All devices were optimized at an annealing temperature of 165 °C. Device characteristics were measured under simulated AM 1.5G irradiation with intensity of 95 mW/cm^2. Error bars denote the standard deviation of the measurements.

The dependence of the overall power conversion efficiency with active layer thicknesses is consistent with more efficient charge extraction from devices with predominantly edge-on P3HT crystallites (5% 1-chloronaphthalene). We observe little changes (~10%) in open-circuit voltages (V_{OC}) with variations in the active layer thickness as shown in Figure 6b. Thus, changes in the device efficiency with the film thickness are mostly a result of the interplay between short-circuit currents (J_{SC}) and fill factors. For face-on (0% 1-chloronaphthalene) P3HT-*b*-PFTBT cells, the short-circuit currents (Figure 6c) and device efficiencies (Figure 6d) increase initially with the active layer thickness likely due to improved light absorption. The efficiency peaks around 2.3% at a film thickness near 65 nm, where a maximum short-circuit current is also found. Beyond this optimum thickness, limitations in charge transport and charge collection, reflected in reduced fill factors (Figure 6a), lead to an immediate drop in both short-circuit currents and overall efficiencies. In the case of edge-on (5% 1-chloronaphthalene) block copolymer solar cells, however, device efficiencies continue to increase with increasing active layer thickness until about 84 nm. Consequently, enhanced charge extraction in block copolymer solar cells with predominantly edge-on crystals (5% 1-chloronaphthalene) enables thicker active layers for efficient photovoltaic operation. In this way, more photons are absorbed to offset losses due to the larger domain size of films cast with 5% 1-chloronaphthalene as we have discussed previously. As a result, P3HT-*b*-PFTBT solar cells with mostly edge-on P3HT crystallites demonstrate similar photovoltaic performance of 2.2% as that of block copolymer devices with mostly face-on crystals.

Our findings contradict a prevalent hypothesis in organic photovoltaics: that face-on orientations are important for vertical charge transport, to maximize charge extraction, and thereby to maximize overall device performance.[26,27,37,63,64] We propose that the dominant orientation of crystallites, either face-on or edge-on, is not crucial for the bulk transport properties in organic solar cells. Instead, a complete picture of the distribution in crystallite orientations might be important for efficient device operation. In solar cells fabricated from 5% 1-chloronaphthalene solutions, P3HT crystals are predominantly edge-on but also have a wide distribution of orientations. As shown in the distribution of the (100) intensities in Figure 2a, a single distribution is present with a full width at half-maximum (fwhm) near 20°. The wide distribution of crystallite orientations in P3HT is ubiquitous.[41−43,65] A broad distribution of predominantly edge-on crystals but with gradually tilted crystallites could be sufficient to form interconnected pathways for charge transport throughout the active layer. Also, a small deflection angle of 5° for fibrils 1.2 μm long (common for P3HT in polymer mixtures[66−68]) would provide a pathway for charges to

DOI: 10.1021/acs.macromol.6b00370
Macromolecules 2016, 49, 4599−4608

vertically traverse a film that is 100 nm thick. Our hypothesis that the broad distribution of crystallites leads to percolating pathways is consistent with high fill factors of 0.6 and above obtained in devices composed of polymer/fullerene mixtures with preferential edge-on orientations.[42] Nevertheless, all device data reported here are from devices with block copolymer active layers, which could promote charge extraction through self-assembled domains that percolate to the electrodes regardless of the crystallite orientation.

For solar cells cast from solutions without solvent additives, a variety of possibilities could explain why it appears that charge extraction is less efficient in our devices with predominantly face-on P3HT crystallites (0% 1-chloronaphthalene) in the active layer. 1-chloronaphthalene has been shown to increase the crystallinity of polymers,[17,18] and as such, devices cast from solutions containing 5% 1-chloronaphthalene may have higher crystallinity and more efficient charge transport. Indeed, integration of the intensities shown in Figure 2a, after correcting with $\sin(\chi)$,[44,45] suggests a factor of 2 enhancement in the crystallinity for films cast from 5% 1-chloronaphthalene solutions, although the population of face-on crystallites is higher by more than 2 orders of magnitude in films cast without 1-chloronaphthalene. In addition, devices without solvent additive treatment (0% 1-chloronaphthalene) exhibit a majority of face-on crystallites and a significant amount of edge-on P3HT crystals, as reflected in the distinct dual populations near 0 and 90° (Figure 2a). It is possible that a random arrangement of face-on and edge-on orientations in the film may result in considerable grain boundaries with large misorientations or lack of tie chains between neighboring crystallites, such that high-angle grain boundaries serve as defects or barriers for transport. Further, the intercrystal connectivity plays a crucial role in transport in polymeric semiconductors.[69−71] Thus, the distinct populations of face-on and edge-on crystallites in films spun-cast without 1-chloronaphthalene may either disrupt the formation of tie chains between crystallites or transport through tie chains, thereby decreasing the charge mobility within P3HT domains.

Another possibility that could explain why devices with face-on crystallites in the active layer exhibit less efficient charge extraction is a possible dependence of the barrier for charge extraction at the anode on the orientation of P3HT crystallites.[72,73] This hypothesis would imply that face-on P3HT crystallites have a higher barrier for charge extraction than edge-on P3HT crystals. Placing the alkyl side chains in between the conjugated backbone and the electrode should reduce electronic coupling between the polymer and anodic contact, potentially suppressing the formation of interfacial barriers from polarization or molecular reorganization processes.[74] Further work is warranted to explore the role of molecular orientation of conjugated polymers on electrode−semiconductor interfacial barriers.

CONCLUSIONS

We have investigated the role of crystal orientations in organic photovoltaics using a fully conjugated block copolymer P3HT-*b*-PFTBT as a model system. We control the orientation of P3HT crystals from mostly face-on to edge-on packing through the application of 1-chloronaphthalene as a solvent additive. Meanwhile, the self-assembled microstructures of block copolymer films remain largely invariant regardless of the addition of 1-chloronaphthalene. With separate control of chain orientation and the active layer morphology, we are able to examine the role of crystallite texturing on photovoltaic device performance. We find that the optimum performance of P3HT-*b*-PFTBT solar cells is independent of the predominant crystalline texture adopted in the active layer. Our results suggest that face-on crystallite orientations in the active layer are not critical for photovoltaic device performance. Instead, we propose that a broad distribution of crystallite orientations and the presence of intercrystal connections may be important for optimizing charge extraction and photovoltaic device operation.

Although this work is limited to block copolymers, our results suggest that the efficacy of out-of-plane charge transport is independent of the crystallite texture in thin films of conjugated polymers, contrary to conventional thinking on the dependence of charge mobilities on crystallite orientation. Significantly perturbing the orientation of crystallites without affecting other variables can be challenging; for example, one approach is to use materials that differ in regioregularity to tune the crystallite orientation from mostly face-on to edge-on,[23] but the regioregularity can also affect crystallization, charge transport, and the morphological evolution in polymer/fullerene mixtures.[66,75] Furthermore, recent evidence has demonstrated that many polymers with high in-plane mobilities (near 1 $cm^2/(V\ s)$) in transistors are not always composed of mostly edge-on crystalline textures in the active layer.[76−79] A possible explanation is that transport is largely one-dimensional along the chain backbone,[79] such that charge hopping between chains for in-plane transport is efficient when both edge-on and face-on orientations are dominant. Here our results demonstrate that even when the transport direction is along a crystallographic direction that is insulating, broad distributions of crystal orientations can lead to efficient transport, likely because of the one-dimensional character of charge transport in conjugated polymers.

ASSOCIATED CONTENT

Supporting Information

The Supporting Information is available free of charge on the ACS Publications website at DOI: 10.1021/acs.macromol.6b00370.

UV−vis absorption spectra of films cast from solutions with and without 1-chloronaphthalene and coherence lengths from GIWAXS data (PDF)

AUTHOR INFORMATION

Corresponding Author

*E-mail edg12@psu.edu (E.D.G.).

Notes

The authors declare no competing financial interest.

ACKNOWLEDGMENTS

Financial support from the Office of Naval Research under Grant N000141410532 is gratefully acknowledged. The Advanced Light Source is an Office of Science User Facility operated for the U.S. Department of Energy Office of Science by Lawrence Berkeley National Laboratory and is supported by the U.S. Department of Energy under Contract DE-AC02-05CH11231. Use of the NSLS is supported by the U.S. Department of Energy, Office of Science, Office of Basic Energy Sciences, under Contract DE-AC02-98CH10886. This research used resources of the Advanced Photon Source, a U.S. Department of Energy (DOE) Office of Science User Facility

DOI: 10.1021/acs.macromol.6b00370
Macromolecules 2016, 49, 4599−4608

operated for the DOE Office of Science by Argonne National Laboratory under Contract DE-AC02-06CH11357.

REFERENCES

(1) Shaheen, S. E.; Ginley, D. S.; Jabbour, G. E. Organic-based photovoltaics. toward low-cost power generation. *MRS Bull.* **2005**, *30*, 10−19.
(2) Gaudiana, R.; Brabec, C. Organic materials - Fantastic plastic. *Nat. Photonics* **2008**, *2*, 287−289.
(3) Forrest, S. R. The path to ubiquitous and low-cost organic electronic appliances on plastic. *Nature* **2004**, *428*, 911−918.
(4) Huang, Y.; Liu, X.; Wang, C.; Rogers, J. T.; Su, G. M.; Chabinyc, M. L.; Kramer, E. J.; Bazan, G. C. Structural Characterization of a Composition Tolerant Bulk Heterojunction Blend. *Adv. Energy Mater.* **2014**, *4*, 1301886.
(5) Bartelt, J. A.; Beiley, Z. M.; Hoke, E. T.; Mateker, W. R.; Douglas, J. D.; Collins, B. A.; Tumbleston, J. R.; Graham, K. R.; Amassian, A.; Ade, H.; Fréchet, J. M. J.; Toney, M. F.; McGehee, M. D. The Importance of Fullerene Percolation in the Mixed Regions of Polymer−Fullerene Bulk Heterojunction Solar Cells. *Adv. Energy Mater.* **2013**, *3*, 364−374.
(6) van Bavel, S. S.; Sourty, E.; de With, G.; Loos, J. Three-Dimensional Nanoscale Organization of Bulk Heterojunction Polymer Solar Cells. *Nano Lett.* **2009**, *9*, 507−513.
(7) Herzing, A. A.; Richter, L. J.; Anderson, I. M. 3D Nanoscale Characterization of Thin-Film Organic Photovoltaic Device Structures via Spectroscopic Contrast in the TEM 1. *J. Phys. Chem. C* **2010**, *114*, 17501−17508.
(8) Roehling, J. D.; Batenburg, K. J.; Swain, F. B.; Moule, A. J.; Arslan, I. Three-Dimensional Concentration Mapping of Organic Blends. *Adv. Funct. Mater.* **2013**, *23*, 2115−2122.
(9) Thompson, B. C.; Fréchet, J. M. J. Polymer−Fullerene Composite Solar Cells. *Angew. Chem., Int. Ed.* **2008**, *47*, 58−77.
(10) Cai, W. Z.; Gong, X.; Cao, Y. Polymer solar cells: Recent development and possible routes for improvement in the performance. *Sol. Energy Mater. Sol. Cells* **2010**, *94*, 114−127.
(11) Hoppe, H.; Sariciftci, N. S. Polymer Solar Cells. In *Photoresponsive Polymers Ii*; Marder, S. R., Lee, K. S., Eds.; Springer: 2008; pp 1−86.
(12) Westacott, P.; Tumbleston, J. R.; Shoaee, S.; Fearn, S.; Bannock, J. H.; Gilchrist, J. B.; Heutz, S.; deMello, J.; Heeney, M.; Ade, H.; Durrant, J. R.; McPhail, D. S.; Stingelin, N. On the Role of Intermixed Phases in Organic Photovoltaic Blends. *Energy Environ. Sci.* **2013**, *6*, 2756−2764.
(13) Subramaniyan, S.; Xin, H.; Kim, F. S.; Shoaee, S.; Durrant, J. R.; Jenekhe, S. A. Effects of Side Chains on Thiazolothiazole-Based Copolymer Semiconductors for High Performance Solar Cells. *Adv. Energy Mater.* **2011**, *1*, 854−860.
(14) Rice, A. H.; Giridharagopal, R.; Zheng, S. X.; Ohuchi, F. S.; Ginger, D. S.; Luscombe, C. K. Controlling Vertical Morphology within the Active Layer of Organic Photovoltaics Using Poly(3-hexylthiophene) Nanowires and Phenyl-C61-butyric Acid Methyl Ester. *ACS Nano* **2011**, *5*, 3132−3140.
(15) Kim, J. B.; Allen, K.; Oh, S. J.; Lee, S.; Toney, M. F.; Kim, Y. S.; Kagan, C. R.; Nuckolls, C.; Loo, Y. L. Small-Molecule Thiophene-C-60 Dyads As Compatibilizers in Inverted Polymer Solar Cells. *Chem. Mater.* **2010**, *22*, 5762−5773.
(16) Yang, X.; Uddin, A. 7 Effect of thermal annealing on P3HT:PCBM bulk-heterojunction organic solar cells: A critical review. *Renewable Sustainable Energy Rev.* **2014**, *30*, 324−336.
(17) Liao, H. C.; Ho, C. C.; Chang, C. Y.; Jao, M. H.; Darling, S. B.; Su, W. F. 8 Additives for morphology control in high-efficiency organic solar cells. *Mater. Today* **2013**, *16*, 326−336.
(18) Chen, L. M.; Hong, Z. R.; Li, G.; Yang, Y. Recent Progress in Polymer Solar Cells: Manipulation of Polymer: Fullerene Morphology and the Formation of Efficient Inverted Polymer Solar Cells. *Adv. Mater.* **2009**, *21*, 1434−1449.
(19) Liu, Y. H.; Zhao, J. B.; Li, Z. K.; Mu, C.; Ma, W.; Hu, H. W.; Jiang, K.; Lin, H. R.; Ade, H.; Yan, H. Aggregation and morphology control enables multiple cases of high-efficiency polymer solar cells. *Nat. Commun.* **2014**, *5*, 5293.
(20) Liu, S. J.; Zhang, K.; Lu, J. M.; Zhang, J.; Yip, H. L.; Huang, F.; Cao, Y. High-Efficiency Polymer Solar Cells via the Incorporation of an Amino-Functionalized Conjugated Metallopolymer as a Cathode Interlayer. *J. Am. Chem. Soc.* **2013**, *135*, 15326−15329.
(21) Zhang, M. J.; Gu, Y.; Guo, X.; Liu, F.; Zhang, S. Q.; Huo, L. J.; Russell, T. P.; Hou, J. H. Efficient Polymer Solar Cells Based on Benzothiadiazole and Alkylphenyl Substituted Benzodithiophene with a Power Conversion Efficiency over 8%. *Adv. Mater.* **2013**, *25*, 4944−4949.
(22) Sivula, K.; Ball, Z. T.; Watanabe, N.; Frechet, J. M. J. Amphiphilic diblock copolymer compatibilizers and their effect on the morphology and performance of polythiophene: Fullerene solar cells. *Adv. Mater.* **2006**, *18*, 206−210.
(23) Sirringhaus, H.; Brown, P. J.; Friend, R. H.; Nielsen, M. M.; Bechgaard, K.; Langeveld-Voss, B. M. W.; Spiering, A. J. H.; Janssen, R. A. J.; Meijer, E. W.; Herwig, P.; de Leeuw, D. M. Two-dimensional charge transport in self-organized, high-mobility conjugated polymers. *Nature* **1999**, *401*, 685−688.
(24) Chang, J. F.; Sun, B. Q.; Breiby, D. W.; Nielsen, M. M.; Solling, T. I.; Giles, M.; McCulloch, I.; Sirringhaus, H. Enhanced mobility of poly(3-hexylthiophene) transistors by spin-coating from high-boiling-point solvents. *Chem. Mater.* **2004**, *16*, 4772−4776.
(25) Brinkmann, M. Structure and Morphology Control in Thin Films of Regioregular Poly(3-hexylthiophene). *J. Polym. Sci., Part B: Polym. Phys.* **2011**, *49*, 1218−1233.
(26) Rand, B. P.; Cheyns, D.; Vasseur, K.; Giebink, N. C.; Mothy, S.; Yi, Y. P.; Coropceanu, V.; Beljonne, D.; Cornil, J.; Bredas, J. L.; Genoe, J. The Impact of Molecular Orientation on the Photovoltaic Properties of a Phthalocyanine/Fullerene Heterojunction. *Adv. Funct. Mater.* **2012**, *22*, 2987−2995.
(27) Kim, J. S.; Park, Y.; Lee, D. Y.; Lee, J. H.; Park, J. H.; Kim, J. K.; Cho, K. Poly(3-hexylthiophene) Nanorods with Aligned Chain Orientation for Organic Photovoltaics. *Adv. Funct. Mater.* **2010**, *20*, 540−545.
(28) Chen, W.; Qi, D. C.; Huang, H.; Gao, X. Y.; Wee, A. T. S. Organic-Organic Heterojunction Interfaces: Effect of Molecular Orientation. *Adv. Funct. Mater.* **2011**, *21*, 410−424.
(29) He, M.; Wang, M. Y.; Lin, C. J.; Lin, Z. Q. Optimization of molecular organization and nanoscale morphology for high performance low bandgap polymer solar cells. *Nanoscale* **2014**, *6*, 3984−3994.
(30) Rivnay, J.; Steyrleuthner, R.; Jimison, L. H.; Casadei, A.; Chen, Z. H.; Toney, M. F.; Facchetti, A.; Neher, D.; Salleo, A. Drastic Control of Texture in a High Performance n-Type Polymeric Semiconductor and Implications for Charge Transport. *Macromolecules* **2011**, *44*, 5246−5255.
(31) Shao, S. Y.; Liu, J.; Zhang, J. D.; Zhang, B. H.; Xie, Z. Y.; Geng, Y. H.; Wang, L. X. Interface-Induced Crystalline Ordering and Favorable Morphology for Efficient Annealing-Free Poly(3-hexylthiophene): Fullerene Derivative Solar Cells. *ACS Appl. Mater. Interfaces* **2012**, *4*, 5704−5710.
(32) Kim, D. H.; Jang, Y.; Park, Y. D.; Cho, K. Layered molecular ordering of self-organized poly(3-hexylthiophene) thin films on hydrophobized surfaces. *Macromolecules* **2006**, *39*, 5843−5847.
(33) Osaka, I.; Saito, M.; Koganezawa, T.; Takimiya, K. Thiophene-Thiazolothiazole Copolymers: Significant Impact of Side Chain Composition on Backbone Orientation and Solar Cell Performances. *Adv. Mater.* **2014**, *26*, 331−338.
(34) Tumbleston, J. R.; Collins, B. A.; Yang, L.; Stuart, A. C.; Gann, E.; Ma, W.; You, W.; Ade, H. The influence of molecular orientation on organic bulk heterojunction solar cells. *Nat. Photonics* **2014**, *8*, 385−391.
(35) Mukherjee, S.; Proctor, C. M.; Tumbleston, J. R.; Bazan, G. C.; Thuc-Quyen, N.; Ade, H. Importance of Domain Purity and Molecular Packing in Efficient Solution-Processed Small-Molecule Solar Cells. *Adv. Mater.* **2015**, *27*, 1105−1111.
(36) Kitchen, B.; Awartani, O.; Kline, R. J.; McAfee, T.; Ade, H.; O'Connor, B. T. Tuning Open-Circuit Voltage in Organic Solar Cells

DOI: 10.1021/acs.macromol.6b00370
Macromolecules 2016, 49, 4599−4608

with Molecular Orientation. *ACS Appl. Mater. Interfaces* **2015**, *7*, 13208−13216.
(37) Guo, C.; Lin, Y.-H.; Witman, M. D.; Smith, K. A.; Wang, C.; Hexemer, A.; Strzalka, J.; Gomez, E. D.; Verduzco, R. Conjugated Block Copolymer Photovoltaics with near 3% Efficiency through Microphase Separation. *Nano Lett.* **2013**, *13*, 2957−2963.
(38) Jiang, Z.; Li, X.; Strzalka, J.; Sprung, M.; Sun, T.; Sandy, A. R.; Narayanan, S.; Lee, D. R.; Wang, J. The dedicated high-resolution grazing-incidence X-ray scattering beamline 8-ID-E at the Advanced Photon Source. *J. Synchrotron Radiat.* **2012**, *19*, 627−636.
(39) Jiang, Z. GIXSGUI: a MATLAB toolbox for grazing-incidence X-ray scattering data visualization and reduction, and indexing of buried three-dimensional periodic nanostructured films. *J. Appl. Crystallogr.* **2015**, *48*, 917−926.
(40) Smith, K. A.; Lin, Y.-H.; Mok, J. W.; Yager, K. G.; Strzalka, J.; Nie, W.; Mohite, A. D.; Verduzco, R. Molecular Origin of Photovoltaic Performance in Donor-*block*-Acceptor All-Conjugated Block Copolymers. *Macromolecules* **2015**, *48*, 8346−8353.
(41) Yang, H.; Shin, T. J.; Yang, L.; Cho, K.; Ryu, C. Y.; Bao, Z. Effect of Mesoscale Crystalline Structure on the Field-Effect Mobility of Regioregular Poly(3-hexyl thiophene) in Thin-Film Transistors. *Adv. Funct. Mater.* **2005**, *15*, 671−676.
(42) Li, G.; Yao, Y.; Yang, H.; Shrotriya, V.; Yang, G.; Yang, Y. "Solvent annealing" effect in polymer solar cells based on poly(3-hexylthiophene) and methanofullerenes. *Adv. Funct. Mater.* **2007**, *17*, 1636−1644.
(43) Woo, C. H.; Thompson, B. C.; Kim, B. J.; Toney, M. F.; Frechet, J. M. J. The Influence of Poly(3-hexylthiophene) Regioregularity on Fullerene-Composite Solar Cell Performance. *J. Am. Chem. Soc.* **2008**, *130*, 16324−16329.
(44) Rivnay, J.; Mannsfeld, S. C. B.; Miller, C. E.; Salleo, A.; Toney, M. F. Quantitative Determination of Organic Semiconductor Microstructure from the Molecular to Device Scale. *Chem. Rev.* **2012**, *112*, 5488−5519.
(45) Baker, J. L.; Jimison, L. H.; Mannsfeld, S.; Volkman, S.; Yin, S.; Subramanian, V.; Salleo, A.; Alivisatos, A. P.; Toney, M. F. Quantification of Thin Film Crystallographic Orientation Using X-ray Diffraction with an Area Detector. *Langmuir* **2010**, *26*, 9146−9151.
(46) Stohr, J. *NEXAFS Spectroscopy*; Springer: New York, 2003.
(47) Germack, D. S.; Chan, C. K.; Hamadani, B. H.; Richter, L. J.; Fischer, D. A.; Gundlach, D. J.; DeLongchamp, D. M. Substrate-Dependent Interface Composition and Charge Transport in Films for Organic Photovoltaics. *Appl. Phys. Lett.* **2009**, *94*, 233303.
(48) Oosterbaan, W. D.; Bolsée, J.-C.; Gadisa, A.; Vrindts, V.; Bertho, S.; D'Haen, J.; Cleij, T. J.; Lutsen, L.; McNeill, C. R.; Thomsen, L.; Manca, J. V.; Vanderzande, D. Alkyl-Chain-Length-Independent Hole Mobility via Morphological Control with Poly(3-alkylthiophene) Nanofibers. *Adv. Funct. Mater.* **2010**, *20*, 792−802.
(49) Wang, H.; Gomez, E. D.; Kim, J.; Guan, Z. L.; Jaye, C.; Fischer, D. A.; Kahn, A.; Loo, Y. L. Device Characteristics of Bulk-Heterojunction Polymer Solar Cells are Independent of Interfacial Segregation of Active Layers. *Chem. Mater.* **2011**, *23*, 2020−2023.
(50) Gann, E.; Young, A. T.; Collins, B. A.; Yan, H.; Nasiatka, J.; Padmore, H. A.; Ade, H.; Hexemer, A.; Wang, C. Soft x-ray scattering facility at the Advanced Light Source with real-time data processing and analysis. *Rev. Sci. Instrum.* **2012**, *83*, 045110.
(51) Virgili, J. M.; Tao, Y. F.; Kortright, J. B.; Balsara, N. P.; Segalman, R. A. Analysis of order formation in block copolymer thin films using resonant soft X-ray scattering. *Macromolecules* **2007**, *40*, 2092−2099.
(52) Guo, C.; Kozub, D. R.; Kesava, S. V.; Wang, C.; Hexemer, A.; Gomez, E. D. Signatures of Multiphase Formation in the Active Layer of Organic Solar Cells from Resonant Soft X-ray Scattering. *ACS Macro Lett.* **2013**, *2*, 185−189.
(53) Liu, G. L.; Ramirez-Hernandez, A.; Yoshida, H.; Nygard, K.; Satapathy, D. K.; Bunk, O.; de Pablo, J. J.; Nealey, P. F. Morphology of Lamellae-Forming Block Copolymer Films between Two Orthogonal Chemically Nanopatterned Striped Surfaces. *Phys. Rev. Lett.* **2012**, *108*, 065502.
(54) Singh, M.; Odusanya, O.; Wilmes, G. M.; Eitouni, H. B.; Gomez, E. D.; Patel, A. J.; Chen, V. L.; Park, M. J.; Fragouli, P.; Iatrou, H.; Hadjichristidis, N.; Cookson, D.; Balsara, N. P. Effect of molecular weight on the mechanical and electrical properties of block copolymer electrolytes. *Macromolecules* **2007**, *40*, 4578−4585.
(55) Albert, J. N. L.; Epps, T. H., III Self-assembly of block copolymer thin films. *Mater. Today* **2010**, *13*, 24−33.
(56) Knoll, A.; Tsarkova, L.; Krausch, G. Nanoscaling of microdomain spacings in thin films of cylinder-forming block copolymers. *Nano Lett.* **2007**, *7*, 843−846.
(57) Kim, S. H.; Misner, M. J.; Xu, T.; Kimura, M.; Russell, T. P. Highly oriented and ordered arrays from block copolymers via solvent evaporation. *Adv. Mater.* **2004**, *16*, 226−231.
(58) Di, Z. Y.; Posselt, D.; Smilgies, D. M.; Papadakis, C. M. Structural Rearrangements in a Lamellar Diblock Copolymer Thin Film during Treatment with Saturated Solvent Vapor. *Macromolecules* **2010**, *43*, 418−427.
(59) Shaw, P. E.; Ruseckas, A.; Samuel, I. D. W. Exciton diffusion measurements in poly(3-hexylthiophene). *Adv. Mater.* **2008**, *20*, 3516−3520.
(60) Bates, F. S.; Fredrickson, G. H. Block copolymers - Designer soft materials. *Phys. Today* **1999**, *52*, 32−38.
(61) Dennler, G.; Scharber, M. C.; Brabec, C. J. Polymer-Fullerene Bulk-Heterojunction Solar Cells. *Adv. Mater.* **2009**, *21*, 1323−1338.
(62) Vajjala Kesava, S.; Dhanker, R.; Kozub, D. R.; Vakhshouri, K.; Choi, U. H.; Colby, R. H.; Wang, C.; Hexemer, A.; Giebink, N. C.; Gomez, E. D. Mesoscopic Structural Length Scales in P3HT/PCBM Mixtures Remain Invariant for Various Processing Conditions. *Chem. Mater.* **2013**, *25*, 2812−2818.
(63) Rathgeber, S.; Perlich, J.; Kuhnlenz, F.; Turk, S.; Egbe, D. A. M.; Hoppe, H.; Gehrke, R. Correlation between polymer architecture, mesoscale structure and photovoltaic performance in side-chain-modified poly(p-arylene-ethynylene)-alt-poly(p-arylene-vinylene): PCBM bulk-heterojunction solar cells. *Polymer* **2011**, *52*, 3819−3826.
(64) Tumbleston, J. R.; Collins, B. A.; Yang, L. Q.; Stuart, A. C.; Gann, E.; Ma, W.; You, W.; Ade, H. The influence of molecular orientation on organic bulk heterojunction solar cells. *Nat. Photonics* **2014**, *8*, 385−391.
(65) Gomez, E. D.; Barteau, K. P.; Wang, H.; Toney, M. F.; Loo, Y.-L. Correlating the scattered intensities of P3HT and PCBM to the current densities of polymer solar cells. *Chem. Commun.* **2011**, *47*, 436−438.
(66) Kozub, D. R.; Vakhshouri, K.; Orme, L. M.; Wang, C.; Hexemer, A.; Gomez, E. D. Polymer Crystallization of Partially Miscible Polythiophene/Fullerene Mixtures Controls Morphology. *Macromolecules* **2011**, *44*, 5722−5726.
(67) Rice, A. H.; Giridharagopal, R.; Zheng, S. X.; Ohuchi, F. S.; Ginger, D. S.; Luscombe, C. K. Controlling Vertical Morphology within the Active Layer of Organic Photovoltaics Using Poly(3-hexylthiophene) Nanowires and Phenyl-C-61-butyric Acid Methyl Ester. *ACS Nano* **2011**, *5*, 3132−3140.
(68) Vakhshouri, K.; Kesava, S. V.; Kozub, D. R.; Gomez, E. D. Characterization of the mesoscopic structure in the photoactive layer of organic solar cells: A focused review. *Mater. Lett.* **2013**, *90*, 97−102.
(69) Kline, R. J.; McGehee, M. D.; Kadnikova, E. N.; Liu, J. S.; Frechet, J. M. J.; Toney, M. F. Dependence of regioregular poly(3-hexylthiophene) film morphology and field-effect mobility on molecular weight. *Macromolecules* **2005**, *38*, 3312−3319.
(70) Vakhshouri, K.; Gomez, E. D. Effect of Crystallization Kinetics on Microstructure and Charge Transport of Polythiophenes. *Macromol. Rapid Commun.* **2012**, *33*, 2133−2137.
(71) Duong, D. T.; Ho, V.; Shang, Z.; Mollinger, S.; Mannsfeld, S. C. B.; Dacuña, J.; Toney, M. F.; Segalman, R.; Salleo, A. Mechanism of Crystallization and Implications for Charge Transport in Poly(3-ethylhexylthiophene) Thin Films. *Adv. Funct. Mater.* **2014**, *24*, 4515−4521.
(72) Duhm, S.; Heimel, G.; Salzmann, I.; Glowatzki, H.; Johnson, R. L.; Vollmer, A.; Rabe, J. P.; Koch, N. Orientation-dependent ionization

DOI: 10.1021/acs.macromol.6b00370
Macromolecules 2016, 49, 4599−4608

energies and interface dipoles in ordered molecular assemblies. *Nat. Mater.* **2008**, *7*, 326−332.
(73) Koch, N.; Elschner, A.; Schwartz, J.; Kahn, A. Organic molecular films on gold versus conducting polymer: Influence of injection barrier height and morphology on current-voltage characteristics. *Appl. Phys. Lett.* **2003**, *82*, 2281−2283.
(74) Mor, G. K.; Le, T. P.; Vakhshouri, K.; Kozub, D. R.; Gomez, E. D. Elemental Mapping of Interfacial Layers at the Cathode of Organic Solar Cells. *ACS Appl. Mater. Interfaces* **2014**, *6*, 19638−19643.
(75) Sivula, K.; Luscombe, C. K.; Thompson, B. C.; Frechet, J. M. J. Enhancing the thermal stability of polythiophene: Fullerene solar cells by decreasing effective polymer regioregularity. *J. Am. Chem. Soc.* **2006**, *128*, 13988−13989.
(76) Takacs, C. J.; Treat, N. D.; Kraemer, S.; Chen, Z.; Facchetti, A.; Chabinyc, M. L.; Heeger, A. J. Remarkable Order of a High-Performance Polymer. *Nano Lett.* **2013**, *13*, 2522−2527.
(77) Rivnay, J.; Toney, M. F.; Zheng, Y.; Kauvar, I. V.; Chen, Z. H.; Wagner, V.; Facchetti, A.; Salleo, A. Unconventional Face-On Texture and Exceptional In-Plane Order of a High Mobility n-Type Polymer. *Adv. Mater.* **2010**, *22*, 4359−4363.
(78) Zhang, X.; Richter, L. J.; DeLongchamp, D. M.; Kline, R. J.; Hammond, M. R.; McCulloch, I.; Heeney, M.; Ashraf, R. S.; Smith, J. N.; Anthopoulos, T. D.; Schroeder, B.; Geerts, Y. H.; Fischer, D. A.; Toney, M. F. Molecular Packing of High-Mobility Diketo Pyrrolo-Pyrrole Polymer Semiconductors with Branched Alkyl Side Chains. *J. Am. Chem. Soc.* **2011**, *133*, 15073−15084.
(79) Zhang, X.; Bronstein, H.; Kronemeijer, A. J.; Smith, J.; Kim, Y.; Kline, R. J.; Richter, L. J.; Anthopoulos, T. D.; Sirringhaus, H.; Song, K.; Heeney, M.; Zhang, W.; McCulloch, I.; DeLongchamp, D. M. Molecular origin of high field-effect mobility in an indacenodithiophene−benzothiadiazole copolymer. *Nat. Commun.* **2013**, *4*, 2238.

DOI: 10.1021/acs.macromol.6b00370
Macromolecules 2016, 49, 4599−4608